

THREE-DIMENSIONAL RAIL COOLING ANALYSIS FOR A
REPETITIVELY FIRED RAILGUN

H. P. LIU

Presented at the
5th Symposium on Electromagnetic
Launch Technology
Eglin AFB, Florida
April 2-5, 1990

Publication No. PR-102
Center for Electromechanics
The University of Texas at Austin
Balcones Research Center
EME 1.100, Building 133
Austin, TX 78758-4497
(512) 471-4496

THREE-DIMENSIONAL RAIL COOLING ANALYSIS FOR A REPETITIVELY FIRED RAILGUN

H.P. Liu
Center for Electromechanics
The University of Texas at Austin
10100 Burnet Bldg. 133
Austin, TX 78758-4497

Abstract: A three-dimensional (3-D) rail cooling analysis for fabrication and demonstration of a stand-alone repetitive fire compulsator driven 9 MJ gun system has been performed to assure the entire rail can be maintained below its thermal limit for multiple shots. The 3-D rail thermal model can predict the temperature, pressure, and convective heat transfer coefficient variations of the coolant along the 10 m long copper rail. The 9-MJ projectiles will be fired every 20 s for 3 min. Water cooling was used in the model for its high cooling capacity. Single liquid phase heat transfer was assumed in the cooling analysis.

For multiple shots, the temperature difference between the rail and the water was enhanced due to accumulated heat in the rail. As a result, the heat removal by water increased from shot-to-shot. The rail temperature initially increased and finally stabilized after a number of shots.

Introduction

Repetitively-fired railguns have recently been a subject of research interest due to their practical applications. Single shot laboratory-tested railguns were previously designed to use rail heat capacity to absorb the joule heating generated by the rail current. For multiple-shot railguns, thermal management becomes very important and active rail cooling is usually required to prevent the bulk rails from being overheated. During railgun firing, the current diffuses into the rails from the outer surfaces. A highly nonuniform current density distribution in the rails is generated, with high current concentration near the breech bore surface and trailing edge of the armature corners. As a result, the temperature distribution in the rails is also highly nonuniform.

Some previous work has been done on rail heating and cooling. Kerrisk [1] developed a two-dimensional (2-D) model to calculate current and thermal diffusion in a rail cross section near the breech subjected to multiple current pulses, to investigate the acceptability criteria of the combination of coolant channel distribution and convective heat transfer coefficient on different railgun repetition rates. Drake and Rathmann [2] solved Maxwell's equations in two dimensions to describe the current diffusion in the rails and commented on the rail thermal survivability of the rail bore surface. Schnurr [3] reported the development of a computer code to predict the combined thermal and current diffusion in rails and found that localized melting at rail corners may occur under full-power conditions. He also indicated that those highly localized melting points should not cause severe problems because they were surrounded by low temperature regions. A 2-D finite-element method was developed by Auton, et. al. [4] to calculate conductor joule heating in electromagnetic launchers with arbitrary geometries and voltage waveforms. Current and temperature distributions in a simplified 2-D rail geometry with consideration of the armature motion were carried out by Nearing and Huerta [5]. They found that localized current reversal may occur

when total rail current decreases. Wu and Sun [6] built a 2-D model using a current-filament method to analyze the current diffusion and subsequent temperature rise for a cross section at the breech. In their model, each rail was configured as a bundle of filaments and current density was assumed uniformly distributed in each filament.

The repetitive fire lightweight railgun, designed by the Center for Electromechanics at The University of Texas at Austin (CEM-UT) is to fire nine continuous shots in 20-s intervals. Rail cooling may not be necessary if the rail size is overdesigned to absorb the diffused heat. Without cooling, rail material becomes weakened at elevated temperatures and more energy will be consumed at high temperature due to the increase of electrical resistivity. With the weight constraint, active water cooling has been proposed to keep the rails from overheating during the repetitive fire. The coolant flows in a direction that is parallel to the bore axis of the railgun. To perform the rail cooling analysis described, variations of coolant temperature and the convective heat transfer coefficient along the coolant passage have to be predicted prior to the calculation of thermal diffusion in the rails. In this paper, the thermal diffusion within the current pulse duration time (about 7 ms) was assumed to be negligible; therefore, the rail temperature distribution at the end of the pulse was used as the initial temperature distribution for the rail in a separated rail thermal model.

Analysis and Results for Side Passages

In the following rail thermal analysis, a 8.9 cm (3.5 in.) circular bore copper rail with constant rail thickness of 2.54 cm (1 in.) is used. Half of a 90° rail is shown in figure 1. The breech region has higher joule heating than the rest of the rail; hence, a 2-D thermal analysis was performed at the breech initially. For the case of the reduced rotor speed at 7,500 rpm, a 10-m gun is required to accelerate a 2.88-kg projectile to 9 MJ kinetic energy at the muzzle. The corresponding gun current profile is plotted in figure 2. Without incorporating cooling, a 2-D current filament model [6] was used to analyze the current diffusion and the consequent joule heating at the breech with the current profile shown. In general, the criterion for the rail thermal design is that the rail temperature should not exceed half of the melting temperature. The 2-D temperature distribution of rails at the breech right after the current pulse satisfied this criterion. Rail temperatures vary significantly within a very narrow exterior surface region due to skin effect. The limitation of computer storage on the CRAY X-MP/24 and assumption of uniform filament size prevent the 2-D filament model from accurately predicting those high temperatures on the rail's exterior boundaries. A quasi 2-D rail inductance and resistance model has been developed at CEM-UT [7] by first modeling the high frequency current distribution on the rail surface and then modeling the one-dimensional (1-D) diffusion of that current into the rails. For the rail with sharp corners, this 1-D current diffusion model (which should provide

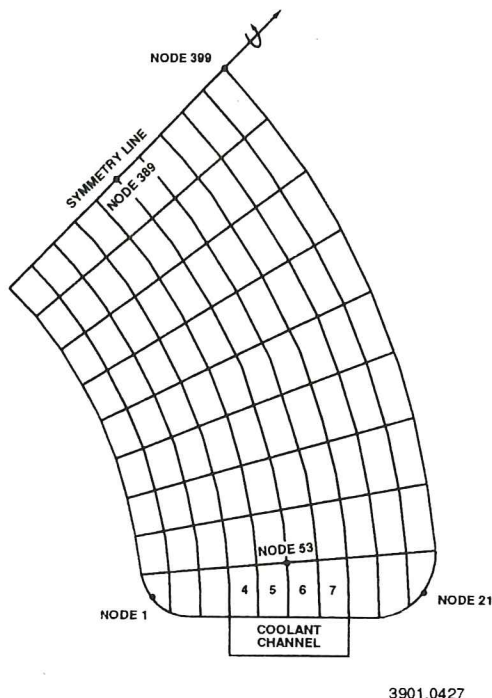


Figure 1. Rail cross section at breech

conservative temperature rise estimates) was used to check the rail surface temperatures. It was found that the temperatures near the corners were unacceptably high. These high corner temperatures can be alleviated by radiusing those corners to relax the field concentration. After a series of analyses, it was determined that both inner and outer corners of the rails should be rounded with a 0.635 cm (0.25 in.) radius curve. For a rail with initial temperature of 293 K, the peak temperature at the radiused inner corners is 911 K which is about 67% of the copper melting temperature. This is 17% over the design criterion, but it is considered to be acceptable because of its very localized and transient nature. This high temperature will be relaxed quickly as the cooling effect is included and should not weaken the material.

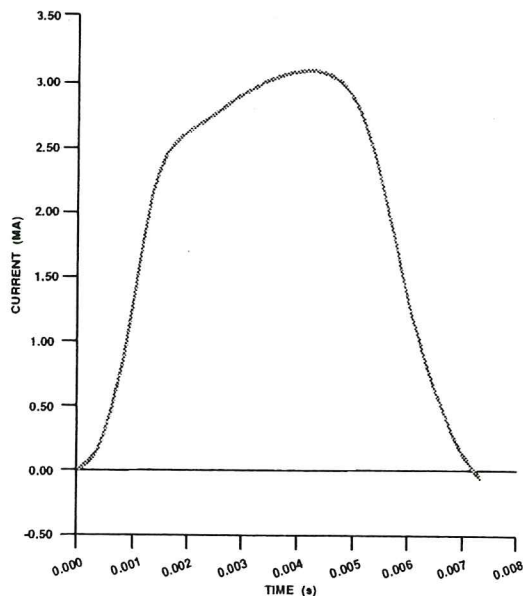


Figure 2. Current profile for a 10-m railgun

A complete 3-D rail cooling analysis using ABAQUS software was performed to assure the entire rail can be maintained below its thermal limit for multiple shots. The 3-D rail thermal model is capable of predicting the temperature and convective heat transfer coefficient variations of the coolant along the rail length. For fully developed turbulent flow in smooth tubes, the following relation [8] was used in the analysis:

$$Nu = 0.023 Re^{0.8} Pr^n$$

where

$$\begin{aligned} Nu &= \text{Nusselt number} \\ Re &= \text{Reynolds number} \\ Pr &= \text{Prandtl number} \\ n &= \begin{cases} 0.4 & \text{for heating} \\ 0.3 & \text{for cooling} \end{cases} \end{aligned}$$

The coolant properties were evaluated at the fluid bulk temperature. A 3-D rail (thermal model) with 1,800 elements was constructed and both inner and outer corners along the entire rail length were rounded with a 0.635 cm (0.25 in.) radius curve. Due to the lack of a 3-D current diffusion model, the initial 3-D temperature distribution (for the cooling analysis) in the rail after a shot must be estimated with certain approximations. The existing 2-D current filament model was used to analyze the current diffusion and subsequent temperature rise at the cross sections down the bore using approximated current waveforms. Time required for a projectile to travel a given distance can be determined from the curve of projectile position vs. time (fig. 3). The current waveform seen by the cross section at the end of the travel will be zeroed during the initial traveling time period, then followed by the remaining gun current waveform. If enough positions along the railgun length are examined this way, a 3-D initial temperature distribution for the cooling analysis can be constructed.

The initial temperature of the thermal model for the cross sections down the bore after the current pulse is introduced, is determined as follows:

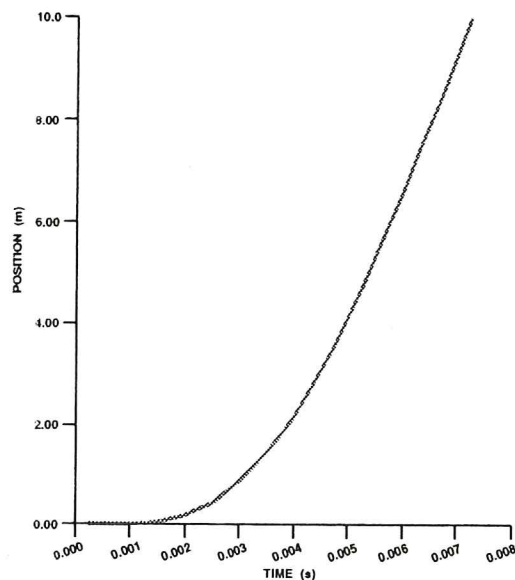
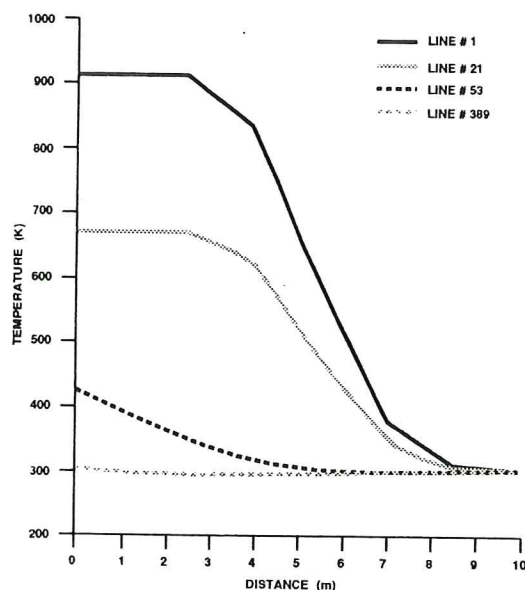


Figure 3. Projectile position vs. time in a 10-m railgun

1. rail temperatures of the surface nodes are calculated by the 1-D current diffusion model and
2. rail temperatures of the interior nodes are calculated by the 2-D current filament model.

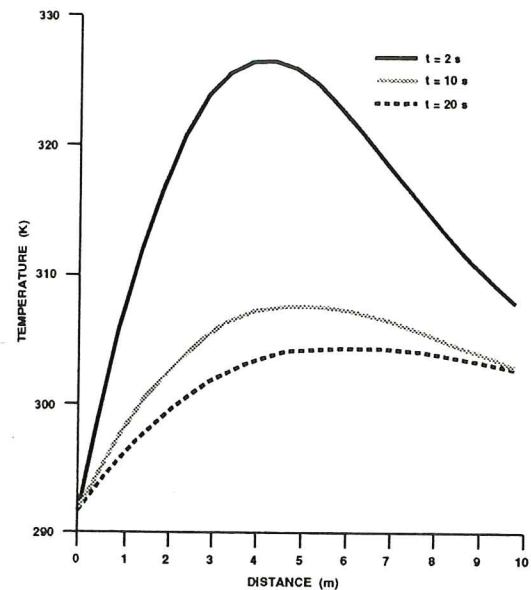
A total of eight cross sections along the rail length were chosen to perform the initial temperature distribution analysis as mentioned above. The locations are the cross section at the breech and cross sections at 1.0, 2.5, 4.0, 5.5, 7.0, 8.5, and 10.0 m from the breech. The 1-D high frequency current diffusion model [7] assumes the input current is a step current pulse. Referring to figures 2 and 3, the current reaches the peak value of 3.1 MA at 4.2 ms and the projectile travels about 2.5 m down the bore during this time period. The peak current of 3.1 MA will eventually be seen by those rail cross sections which are within the distance of 2.5 m from the breech. Therefore, from a conservative point of view, 3.1 MA is used as the step current pulse input in the 1-D current diffusion analysis for the cross sections which are within the distance of 2.5 m from the breech. For any other cross sections down the bore, the input current will be chosen at the time which is required for the projectile to travel to that cross section.

For positions not included in these eight cross sections, rail temperatures were calculated by linear interpolation between those sections with known temperatures. The initial temperature distributions for several representative lines, which are parallel to the bore axis and start with the node numbers shown in figure 1, are included in figure 4. With this 3-D highly nonuniform temperature distribution, it is difficult to determine the amount of energy deposited in the rails. The approach adopted was to perform a 3-D thermal diffusion calculation in the rail and allow no heat transfer across the rail boundaries, resulting eventually in a uniform temperature distribution. The energy deposition can then be calculated by comparing the rail heat content at this temperature with that at the initial temperature of 293 K. By doing so, a 4.11 MJ energy was determined.



3901.0431

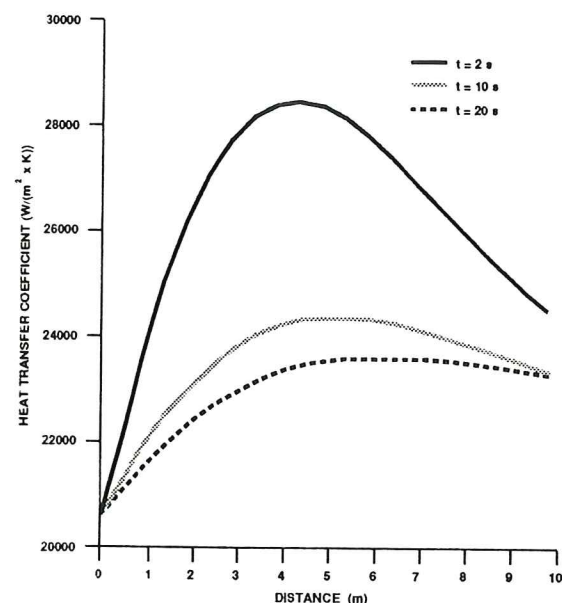
Figure 4. Initial temperature distributions (from breech to muzzle) immediately after first shot



3901.0432

Figure 5. Transient water temperature vs. rail position after first shot

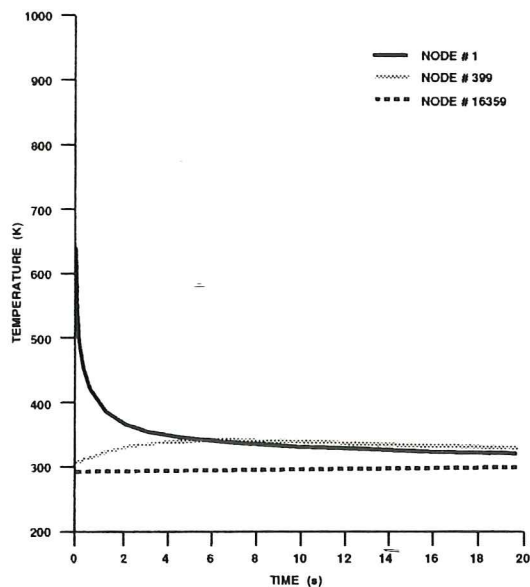
Referring to figure 1, the inner and outer radii are 4.45 cm (1.75 in.) and 6.99 cm (2.75 in.), respectively, and the weight of both rails (with sharp corners) is 408 kg for a 10 m long railgun. The location of the coolant passages is between the rail and insulator, with the size of each coolant passage being 1.016 x 0.381 cm (0.4 x 0.15 in.). As shown in figure 1, the right sides of the elements #4, 5, 6, and 7 are in contact with the coolant. The water flow rate of 0.151 m³ (40 gal) for 3 min providing an inlet velocity of 5.4 m/s was assumed in the analysis. The inlet temperature and pressure of the water were 293 K and 250 psia, respectively. Single phase heat transfer was assumed in the cooling analysis. The resulting transient water temperature and convective heat transfer coefficient variations along the coolant channel are plotted in figures 5 and 6. Indications



3901.0433

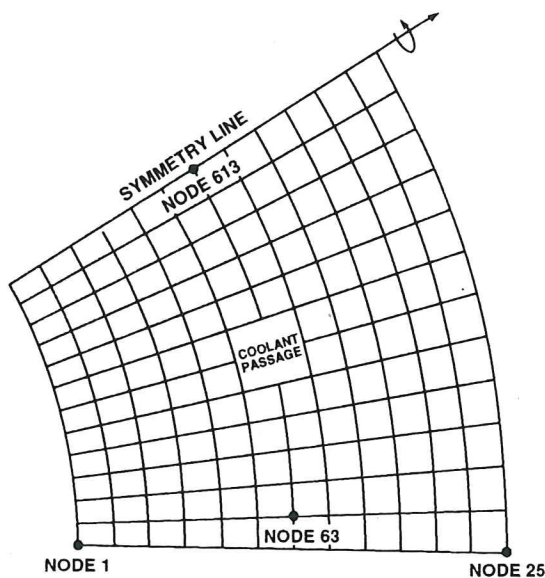
Figure 6. Transient convective heat transfer coefficient vs. rail position after first shot

are the water actually begins to transfer heat back to the rail after 4 m down the bore. Pressure drop across the 10-m passage is about 90 psi. The rail transient temperature distributions at nodes #1, 399, and 16,359 are plotted in figure 7. The nodes #1 and 399 are shown in figure 1 and the node #16,359 (corresponding to node #399 at breech) is located at the muzzle cross section.



3901.0434

Figure 7. Transient rail temperature distributions at several representative nodes after first shot



3901.0435

Figure 8. Approximate half rail cross section at muzzle

After a 20 s cooling period, the temperature in the rail varies from 301.5 to 327.2 K and the energy removed by the coolant is 1.206 MJ (which is about 30% of the energy deposited in the rails). The majority of the heat transfer occurs within the initial 2 to 3 s when large temperature differences exist between the rail boundary and coolant. The bulk of the heat is absorbed by the interior of the rail which has a much lower temperature. After a short period of time, the heat transfer from the rail to the water is

decreased significantly due to the reduced temperature difference. It is expected that the heat removal by water will increase from shot to shot because the temperature difference between rail and water will increase due to accumulated heat in the rail. Rail temperature may initially increase and finally stabilize after a certain number of shots.

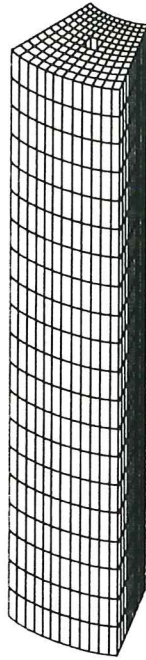
A similar 3-D simulation, which assumed a 4 m long coolant channel from the breech, has been performed. As a result, the heat reversal from water to rail in the previous case was eliminated and approximately 40% of the 4.11 MJ can be removed by the water. Certainly, the impact of this water exit (near the middle of the gun length) on the structural design must be addressed.

Analysis and Results for Internal Passages

In the previous cooling analyses, the rail coolant passage was located between the rail and the insulator to avoid degrading the rail structural stiffness. The potential problem with this side passage is the seal for the coolant. Recently, both the rail structure analysis with the internal coolant passage included and rail fabrication technique have been examined in a detailed manner. The analysis determined the rail outer contour should be smooth enough to prevent stress concentration and the internal coolant passage is allowable only to a certain size (about 1-cm diameter).

An approximate half of a 64.8° copper rail cross section is shown in figure 8, the inner and outer radii are 4.45 cm (1.75 in.) and 8.49 cm (3.34 in.), respectively, and a 3-D rail (axial length is not to scale) with 2,800 elements is shown in figure 9. The rail surface and interior temperatures were previously calculated by the 1-D high frequency model and 2-D current filament model, respectively. High rail surface temperatures (especially near the rail corners) are more likely to be overpredicted by the 1-D model according to the experiences from past CEM-UT railgun experiments. Hence, the 2-D current filament model was used to generate the temperatures for both the surface and interior nodes in the following analysis. Coolant enters the passage at the muzzle and flows all the way to the breech because this cooling scheme can remove heat more effectively in comparison with coolant flowing from breech to muzzle as previously described. The initial temperature distributions immediately after the first shot for several representative lines, which are parallel to the bore axis and started with the node numbers at the muzzle section shown in figure 8, are included in figure 10. As shown in figure 10, the highest temperature occurs at the section about 1 m from the breech due to fast current rising seen by this section (high frequency effect). After the first shot, the energy deposition in both rails was determined as 2.869 MJ.

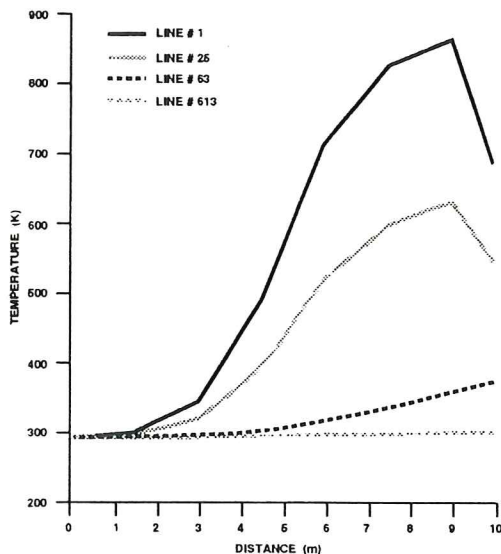
To save coolant consumption, a water flow rate of 0.114 m³ (30 gal) for 3 min was used in the simulation, which provided an inlet velocity of 3.84 m/s. The inlet temperature and pressure of the water were 293 K and 250 psia, respectively. Single phase heat transfer was assumed in the cooling analysis. After the first shot, the resulting transient water temperature and convective heat transfer coefficient variations along the coolant passage are plotted in figures 11 and 12. Referring to figure 11, it can be found that the water almost does not absorb heat in the initial 4 m traveling distance because of the low rail temperature near



3901.0436

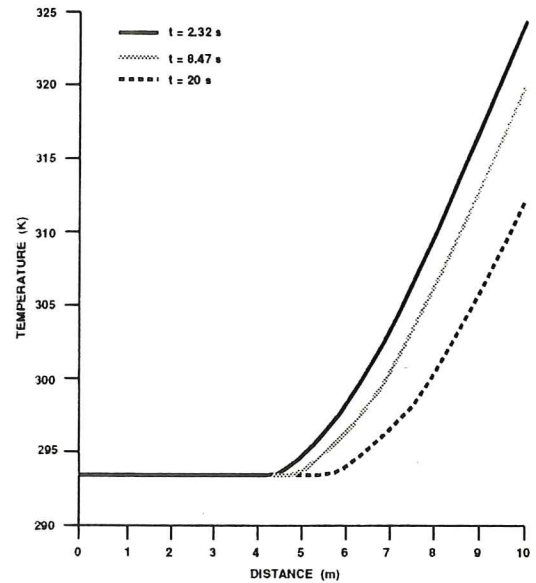
Figure 9. Three-dimensional rail thermal model

the muzzle. Therefore, the coolant can be introduced at the rail axial position of 4 m from the muzzle, if it is possible from the structural and practical viewpoints. The water pressure drop across the 10-m passage is about 41 psi, which is insensitive to the water temperature change across the passage. Rail transient temperature at the breech deserves a detailed examination because the breech has the highest energy deposition from the joule heating and hottest coolant temperature compared to other rail sections. The rail temperature histories at the breech for nodes #25,001; 25,025; 25,063; and 25,613, which correspond to nodes #1, 25, 63, and 613 at the muzzle, respectively, as shown in figure 8, are plotted in figure 13. As shown in figure 13, the temperature distribution at the breech is quite uniform after 20 s thermal diffusion and cooling.



3901.0437

Figure 10. Initial temperature distribution (from muzzle to breech) immediately after first shot

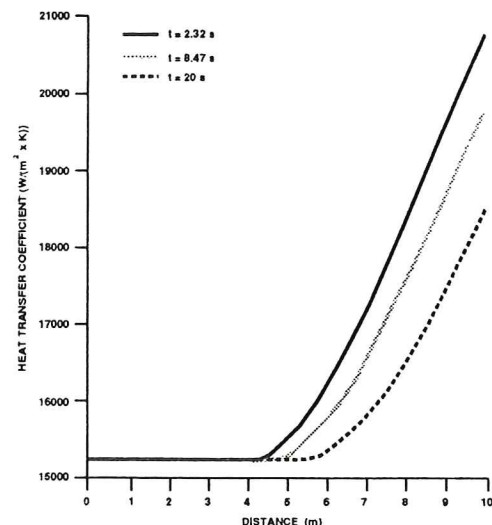


3901.0438

Figure 11. Transient water temperature vs. rail position after first shot

After a 20 s cooling period, the energy removed by the coolant is 1.285 MJ (which is about 44.8% of the energy deposited in the rail). Within this period of time, quick radial heat diffusion makes the temperature distribution in each rail section quite uniform, but the low temperature region near the muzzle absorbs almost no heat from the breech due to the lengthy thermal diffusion path.

Simulating rail cooling for multiple shots has been attempted. After a 20 s cooling period for a certain shot, the relaxed and nonuniform 3-D rail temperature distribution was used as the initial temperature distribution for the next shot to perform the current diffusion, rail temperature rise calculation, and subsequent 20 s water cooling analysis. Rail cooling analyses for the initial four railgun shots have been attempted. For these four consecutive shots, the energy deposition, energy removed by the water, and percentage of deposited energy removed for both rails are summarized in table 1. The temperature extremes at nodes #22,501 (inner corner at the cross section 1 m from the



3901.0439

Figure 12. Transient convective heat transfer coefficient vs. rail position after first shot

breech) and 25,001 (inner corner at breech) are included in table 2. From table 1, it indicates that the energy deposition stabilizes within four shots and the energy removed by the water increases from 44.8% after the first shot to 89.8% after the fourth shot. From table 2, it is obvious that the temperatures of these two hot spots approach their limits after several shots.

Table 1. Energy deposited and removed in both rails

Shot Number	Energy Deposited E_D (MJ)	Energy Removed E_R (MJ)	E_R/E_D
1	2.869	1.285	0.448
2	3.109	2.145	0.690
3	3.156	2.604	0.825
4	3.169	2.845	0.898

Table 2. Temperature extremes after each shot for two representative nodes

Shot Number	T_{22501} (K)	T^*_{22501} (K)	T_{25001} (K)	T^*_{25001} (K)
1	855.2	315.5	680.7	321.4
2	878.1	328.6	705.7	339.3
3	891.3	335.8	721.3	349.5
4	898.4	339.5	730.2	355.1

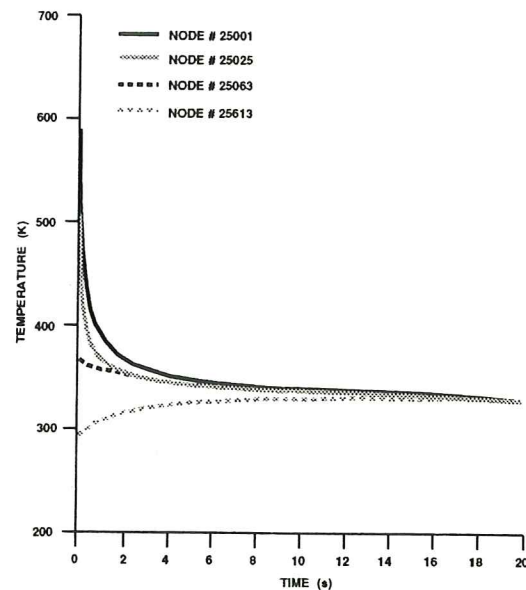
T_{22501} = temperature of node #22501 immediately after a given shot
 T^*_{22501} = temperature of node #22501 at the end of the 20 s cooling period after a given shot

T_{25001} = temperature of node #25001 immediately after a given shot
 T^*_{25001} = temperature of node #25001 at the end of the 20 s cooling period after a given shot

Conclusions

A 3-D rail thermal diffusion model with varied coolant temperature and convective heat transfer coefficient along the rail length has been constructed to analyze transient rail temperature distribution for multiple shots. Due to the lack of a 3-D current diffusion model, the initial 3-D temperature distribution (for the cooling analysis) in the rail after a shot was estimated with an existing 2-D current filament model. The current diffusion and subsequent temperature rise at the cross sections down the bore were analyzed using approximated current waveforms. Simulations demonstrate the water would be heated and would begin to transfer heat back to the rail after 4 m of rail length if the cooling water was introduced at the breech. To avoid this heat reversal, an alternative of flowing water from muzzle to breech has been investigated because the rail temperatures increased from muzzle to breech except for very localized high frequency effect.

For the proposed rail cooling with 20 s between shots, both cooling schemes will work, but flowing coolant from muzzle to breech is desirable because of its efficient heat removal. For the case demanding higher repetition rate (i.e., 1 Hz or more), the coolant should be introduced at breech to achieve maximal heat transfer in this critical area where cooling is needed most.



3901.0440

Figure 13. Transient rail temperature distributions at several representative nodes at breech after first shot

Acknowledgments

The author wishes to thank Albert Wu and Richard Cook for the use of their computer codes to calculate the rail temperature rise due to joule heating. Technical support from Alan Walls, Ray Zowarka, and Professor Bill Weldon are also greatly appreciated. This research is sponsored by the Defense Advanced Research Projects Agency and the U.S. Army Research, Development, and Engineering Center under contract number DAAA21-86-C-0281. Computing resources for this work were provided by The University of Texas System Center for High Performance Computing.

References

- [1] J. F. Kerrisk, "Railgun Conductor Heating from Multiple Current Pulses," *IEEE Transactions on Magnetics*, vol MAG-22, no. 6, November 1986, pp. 1561-1566.
- [2] P. A. Drake and C. E. Rathmann, "Two-Dimensional Current Diffusion in an EML Rail with Constant Properties," *IEEE Transactions on Magnetics*, vol MAG-22, no. 6, November 1986, pp. 1448-1452.
- [3] N. M. Schnurr, "Thermal Analysis of Electromagnetic Launcher Rails," Los Alamos National Laboratory report LA-11087-MS, October 1987.
- [4] J. R. Auton, C. R. Grant, R. L. Houghton, and H. P. Thompson, "A Finite-Element Method for the Prediction of Joule Heating of Conductors in Electromagnetic Launchers," *IEEE Transactions on Magnetics*, vol 25, no. 1, January 1989, pp. 63-67.
- [5] J. C. Nearing and M. A. Huerta, "Skin and Heating Effects of Railgun Current," *IEEE Transactions on Magnetics*, vol 25, no. 1, January 1989, pp. 381-386.
- [6] A. Y. Wu and K. S. Sun, "Formulation and Implementation of the Current Filament Method for the Analysis of Current Diffusion and Heating in Conductors in Railguns and Homopolar Generators," *IEEE Transactions on Magnetics*, vol 25, no. 1, January 1989, pp. 610-615.
- [7] R. W. Cook, "Instruction for Running the High Frequency Inductance Code," CEM-UT Technical Note TN-36, Center for Electromechanics at The University of Texas at Austin, May 1988.
- [8] J. P. Holman, *Heat Transfer*, 5th ed., McGraw-Hill, New York, 1981.